Published in final edited form as:
IEEE Antennas Wirel Propag Lett. 2012 ; 11: 1610–1613. doi:10.1109/LAWP.2012.2236293.

MRI-Derived 3-D-Printed Breast Phantom for Microwave Breast Imaging Validation

Matthew J. Burfeindt [Student Member, IEEE], **Timothy J. Colgan [Student Member, IEEE]**, **R. Owen Mays [Student Member, IEEE]**, **Jacob D. Shea [Member, IEEE]**, **Nader Behdad [Member, IEEE]**, **Barry D. Van Veen [Fellow, IEEE]**, and **Susan C. Hagness [Fellow, IEEE]**
Department of Electrical and Computer Engineering, University of Wisconsin–Madison, Madison, WI 53706 USA

Abstract

We propose a 3-D-printed breast phantom for use in preclinical experimental microwave imaging studies. The phantom is derived from an MRI of a human subject; thus, it is anthropomorphic, and its interior is very similar to an actual distribution of fibroglandular tissues. Adipose tissue in the breast is represented by the solid plastic (printed) regions of the phantom, while fibroglandular tissue is represented by liquid-filled voids in the plastic. The liquid is chosen to provide a biologically relevant dielectric contrast with the printed plastic. Such a phantom enables validation of microwave imaging techniques. We describe the procedure for generating the 3-D-printed breast phantom and present the measured dielectric properties of the 3-D-printed plastic over the frequency range 0.5–3.5 GHz. We also provide an example of a suitable liquid for filling the fibroglandular voids in the plastic.

Keywords

Microwave imaging; phantoms

I. Introduction

MICROWAVE breast imaging via inverse scattering involves reconstructing the distribution of dielectric properties within the breast volume from measured scattered electric fields. The dielectric properties distribution conveys anatomical and functional information about the underlying tissue composition due to the dielectric contrast between different types of tissue in the breast [1]. Quantitative validation is crucial for both development and performance evaluation of microwave breast-imaging techniques. Image validation involves comparing the estimated dielectric profile to the actual profile of the object under test in order to ascertain accuracy in the reconstructed values and their spatial distribution throughout the interior of the object.

(bmatthew@wisc.edu; tcolgan@wisc.edu; rmays@wisc.edu; jake.shea@elemenllc.com; behdad@engr.wisc.edu; vanveen@engr.wisc.edu; hagness@engr.wisc.edu)..

Clinical imaging with human subjects [2], [3] provides the most faithful test domain. However, the lack of knowledge of the true *in vivo* dielectric distribution limits the extent to which microwave imaging techniques may be validated in a clinical setting. Numerical studies using MRI-derived numerical breast phantoms (e.g., [4]–[6]) serve as a powerful testbed for evaluating imaging techniques, as the reconstructed dielectric profiles can be compared directly and unambiguously to the true object, which is realistic in both dielectric properties and interior structure. Numerical studies do not, however, introduce the complications inherent in experimental imaging, such as imperfect antenna modeling and environmental interference. Realistic experimental breast phantoms are therefore a critical component of preclinical validation of microwave breast-imaging techniques.

Several previous studies have reported experimental phantoms that have anthropomorphic exterior surfaces and are constituted by synthetic materials that approximate (to varying degrees of accuracy) the dielectric properties of skin, fibroglandular, and adipose tissue. These phantoms have interiors that are either homogeneous (e.g., adipose-tissue simulant enclosed by a thin layer of skin simulant) [7], homogeneous except for a target inclusion (e.g., malignant-tissue simulant) [8], [9], or heterogeneous [10]–[12]. Heterogeneity is achieved by distributing fibroglandular tissue simulants nonuniformly in the phantom interior. In the examples of [10] and [12], a high degree of dielectric properties realism is achieved through the use of tissue-mimicking oil-in-gelatin dispersions [13]. However, it is difficult to use the phantom construction methods of [10]-[12] to distribute fibroglandular tissue simulants throughout the adipose-tissue simulant in such a way as to realistically mimic the structural complexity of the interior of the breast. Experimental phantoms that provide a more accurate representation of the interior breast structure, even if at the expense of dielectric properties accuracy, will play an important complementary role in validating the ability of microwave imaging strategies to resolve realistic structural features of breast tissue.

Recent advances in three-dimensional (3-D) rapid prototyping technology allow the printing of highly complex plastic objects from precise computer models. In this letter, we propose an MRI-derived 3-D-printed breast phantom for experimental validation of microwave breast imaging. The portion of the model that is printed in plastic corresponds to locations of adipose tissue, while the void in the model corresponds to locations of fibroglandular tissue. Both the exterior and interior of the model are derived from an MRI of a human subject. Thus, the exterior is anthropomorphic, while the interior spatial layout of the void within the plastic is correlated strongly with a realistic distribution of fibroglandular tissue surrounded by adipose tissue. The void is filled with a liquid that provides a biologically relevant dielectric contrast with the plastic—one that mimics the contrast between fibroglandular and adipose tissue. Additionally, the exterior surface of the phantom may be coated with a tissue-mimicking material for skin such as that proposed in [12] and [13], and a small object may be suspended in the liquid-filled region to mimic a malignant tumor in fibroglandular tissue. The 3-D-printed phantom is thus a promising test object for validating microwave inverse scattering techniques and systems designed for microwave breast imaging. In the following sections, we describe the procedure for constructing the 3-D-printed breast

phantom, present the dielectric properties of the 3-D-printed plastic and an example liquid with which to fill the void, and make concluding comments.

II. Phantom Construction

The 3-D-printed breast phantom was derived from a heterogeneously dense (Class III in terms of BI-RADS density) numerical breast phantom in the University of Wisconsin Computational Laboratory (UWCEM) breast phantom repository [14]. The numerical phantom is MRI-derived and is thus anthropomorphic and heterogeneous with realistic interior tissue structure. Coronal cross sections through the dielectric profile of the numerical phantom are shown in Fig. 1 (top row).

Constructing the printed phantom model involves creating a volumetric binary mask that differentiates between solid plastic and air void regions. This requires removing the numerical phantom's skin layer and segmenting the fibroglandular regions from the adipose regions. However, simply thresholding the numerical phantom to identify regions of fibroglandular tissue may lead to the erroneous creation of noncontiguous solid regions that fall out of the phantom and/or to noncontiguous isolated voids that cannot be filled with liquid.

We avoided this problem by convolving the distribution of Debye parameter ε_s (static permittivity) with a spherical Gaussian blurring function of variance 25 mm^2 and support radius of 4.5 mm. Fig. 1 (middle row) shows cross sections through the blurred dielectric distribution. We then thresholded the blurred numerical phantom at $\varepsilon_s = 15$. Voxels below the threshold (that is, voxels nearest to adipose tissue in dielectric properties) were designated as belonging to the solid part of the model, while voxels above the threshold (that is, voxels nearest to fibroglandular tissues in dielectric properties) were designated as belonging to the void. Cross sections through the resulting binary phantom model are shown in Fig. 1 (bottom row). The binary model is very heterogeneous; the void regions preserve the location and shape of fibroglandular tissue structures in the original phantom, albeit with a slightly reduced spatial resolution. All void regions are contiguous, allowing them to be filled with a single liquid solution.

A slab of dimensions $146 \times 132 \times 5$ mm^3 was added to the posterior base of the model. The slab enables positioning the printed breast phantom in a microwave antenna array such as the one described in [15].

Three-dimensional printers typically require computer models in the form of a series of two-dimensional (2-D) facets that describe the surfaces composing the object to be printed. We used the volumetric binary breast model (e.g., bottom of Fig. 1) to generate a series of surface facets representing both the outer surface of the phantom and the surface of the interior void. The facet model was then exported to a Dimension Elite 3-D Printer (Dimension, Inc., Eden Prairie, MN), which printed the phantom using acrylonitrile butadiene styrene (ABS) plastic. The nominal spatial resolution of the 3-D printer is between 0.178 and 0.254 mm, which is at least two orders of magnitude smaller than the wavelength in the UHF band. The printing process took approximately 36 h. Photographs of the resulting 3-D-printed breast phantom prior to filling the air voids with liquid are shown

in Fig. 2. The file exported to the 3-D printer is made available to the scientific community via the UWCEM breast phantom repository at http://uwcem.ece.wisc.edu.

III. Dielectric Characterization of Phantom Materials

Knowledge of the dielectric properties of the materials constituting the phantom is important for quantitative evaluation of the resulting microwave images of the phantom. We characterized the dielectric properties of the 3-D-printed ABS plastic using the technique described in [16]. First, we 3-D-printed a slab of ABS plastic of dimensions $200 \times 100 \times 2$ mm^3. We then fabricated a microstrip transmission line of length 200 mm and width 6 mm on the plastic slab. SMA connectors were soldered to both ends of the transmission line, and *S*-parameter measurements were made using an Agilent E8364 vector network analyzer. Agilent's commercial software package Advanced Design System (ADS) was then used to create a simulated microstrip transmission-line model. The permittivity and loss tangent of the simulated microstrip line were optimized in ADS at 0.5-GHz intervals to obtain a good match between simulation and measurement. The process was repeated for five different transmission lines. The resulting estimated dielectric constant and effective conductivity are plotted in Fig. 3 over the frequency range of interest for quantitative microwave breast tomography (0.5–3.5 GHz). Data points correspond to the mean over the five transmission lines and error bars span the maximum and minimum values. The dielectric constant is around 2.25 across the entire frequency range, while the effective conductivity ranges from a minimum of 1.7 mS/m at 0.75 GHz to a maximum of 5.9 mS/m at 3.25 GHz.

An example of a liquid with which to fill the void is a solution of Triton X-100 surfactant and deionized water. Such solutions have been proposed previously to mimic the dielectric properties of biological tissues [17]. A biologically relevant contrast between the plastic and the solution can be obtained by choosing an appropriate ratio between Triton and deionized water. For demonstrative purposes, we measured the dielectric properties of a 90%–10% solution of Triton and deionized water using the coaxial probe technique described in [18]. The Triton solution has a dielectric constant ranging from about 8.1 at 0.5 GHz to about 5.4 at 3.5 GHz. The effective conductivity ranges from about 71 mS/m at 0.5 GHz to about 390 mS/m at 3.5 GHz. The magnitude of the ratio of intrinsic impedance between the Triton solution and the printed plastic is about 0.58 at 2 GHz. This is comparable to the magnitude of the ratio of intrinsic impedance between 25th-percentile fibroglandular tissue and 75th-percentile adipose tissue at 2 GHz, which is 0.45 using the Cole–Cole models reported in [14].

IV. Conclusion

In this letter, we proposed an MRI-derived, 3-D-printed breast phantom for use in microwave breast-imaging experiments. The interior structure of the phantom is very similar to a realistic distribution of fibroglandular and adipose tissue. The void of the 3-D-printed model can be filled with a dispersive liquid in order to provide a biologically relevant dielectric contrast with the printed plastic, while a small object may be suspended in the liquid to approximate the presence of a tumor in fibroglandular tissue. Microwave images can be compared directly to the 3-D binary model used for printing the phantom, permitting

unambiguous coregistration between the phantom interior structure and the reconstructed dielectric profile. Rigorous experimental validation of microwave imaging techniques is made possible with these 3-D printed phantoms due to the availability of the exact structure as well as the dielectric properties, as characterized here.

Acknowledgments

This work was supported by the Department of Defense SMART Scholarship for Service Program and the National Institutes of Health under Grant R21 CA161369.

References

1. Lazebnik M, Popovic D, McCartney L, Watkins C, Lindstrom M, Harter J, Sewall S, Ogilvie T, Magliocco A, Breslin T, Temple W, Mew D, Booske J, Okoniewski M, Hagness S. A large-scale study of the ultrawideband microwave dielectric properties of normal, benign and malignant breast tissues obtained from cancer surgeries. Phys. Med. Biol. 2007; 52:6093–6115. [PubMed: 17921574]
2. Meaney P, Fanning M, Raynolds T, Fox C, Fang Q, Kogel C, Poplack S, Paulsen K. Initial clinical experience with microwave breast imaging in women with normal mammography. Acad. Radiol. 2007; 14(2):207–218. [PubMed: 17236994]
3. Poplack S, Tosteson T, Wells W, Pogue B, Meaney P, Hartov A, Kogel C, Soho S, Gibson J, Paulsen K. Electromagnetic breast imaging: Results of a pilot study in women with abnormal mammograms. Radiology. 2007; 243(2):350–359. [PubMed: 17400760]
4. Winters D, Shea J, Kosmas P, Van Veen B, Hagness S. Three-dimensional microwave breast imaging: Dispersive dielectric properties estimation using patient-specific basis functions. IEEE Trans. Med. Imag. Jul; 2009 28(7):969–981.
5. Johnson J, Takenaka T, Ping K, Honda S, Tanaka T. Advances in the 3-D forward-backward time-stepping (FBTS) inverse scattering technique for breast cancer detection. IEEE Trans. Biomed. Eng. Sep; 2009 56(9):2232–2243. [PubMed: 19457739]
6. Shea J, Kosmas P, Hagness S, Van Veen B. Three-dimensional microwave imaging of realistic numerical breast phantoms via a multiple-frequency inverse scattering technique. Med. Phys. 2010; 37:4210–4226. [PubMed: 20879582]
7. Winters D, Shea J, Madsen E, Frank G, Van Veen B, Hagness S. Estimating the breast surface using UWB microwave monostatic backscatter measurements. IEEE Trans. Biomed. Eng. Jan; 2008 55(1):247–256. [PubMed: 18232368]
8. Miyakawa, M.; Takata, S.; Inotsume, K. Development of non-uniform breast phantom and its microwave imaging for tumor detection by CP-MCT; Proc. Annu. Int. Conf. IEEE EMBS, Minneapolis, MN; 2009. p. 2723-2726.
9. Golnabi, A.; Meaney, P.; Epstein, N.; Paulsen, K. Microwave imaging for breast cancer detection: Advances in three-dimensional image reconstruction; Proc. Annu. Int. Conf. IEEE EMBS, Prague, Czech Republic; 2011. p. 5730-5733.
10. Croteau, J.; Sill, J.; Williams, T.; Fear, E. Phantoms for testing radar-based microwave breast imaging; Proc. 13th Int. Symp. Antenna Technol. Appl. Electromagn. Canadian Radio Sci. Meeting, Toronto, ON, Canada; 2009. p. 1-4.
11. Klemm M, Leendertz J, Gibbins D, Craddock I, Preece A, Benjamin R. Microwave radar-based breast cancer detection: Imaging in inhomogeneous breast phantoms. IEEE Antennas Wireless Propag. Lett. 2009; 8:1349–1352.
12. Mashal A, Gao F, Hagness S. Heterogeneous anthropomorphic phantoms with realistic dielectric properties for microwave breast imaging experiments. Microw. Opt. Technol. Lett. 2011; 53(8): 1896–1902. [PubMed: 21866208]
13. Lazebnik M, Madsen E, Frank G, Hagness S. Tissue-mimicking phantom materials for narrowband and ultrawideband microwave applications. Phys. Med. Biol. 2005; 50(18):4245. [PubMed: 16148391]

14. Zastrow E, Davis S, Lazebnik M, Kelcz F, Van Veen B, Hagness S. Development of anatomically realistic numerical breast phantoms with accurate dielectric properties for modeling microwave interactions with the human breast. IEEE Trans. Biomed. Eng. Dec; 2008 55(12):2792–2800. [PubMed: 19126460]

15. Aguilar, S.; Al-Joumayly, M.; Shea, J.; Behdad, N.; Hagness, S. Design of a microwave breast imaging array composed of dual-band miniaturized antennas; Proc. 30th URSI Gen. Assembly Sci. Symp., Istanbul, Turkey; 2011. p. 1-4.

16. Aguilar S, Shea J, Al-Joumayly M, Van Veen B, Behdad N, Hagness S. Dielectric characterization of PCL-based thermoplastic materials for microwave diagnostic and therapeutic applications. IEEE Trans. Biomed. Eng. Mar; 2012 59(3):627–633. [PubMed: 21622068]

17. Romeo S, Di Donato L, Bucci O, Catapano I, Crocco L, Scarfì M, Massa R. Dielectric characterization study of liquid-based materials for mimicking breast tissues. Microw. Opt. Technol. Lett. 2011; 53(6):1276–1280.

18. Popovic D, McCartney L, Beasley C, Lazebnik M, Okoniewski M, Hagness S, Booske J. Precision open-ended coaxial probes for in vivo and ex vivo dielectric spectroscopy of biological tissues at microwave frequencies. IEEE Trans. Microw. Theory Tech. May; 2005 53(5):1713–1722.

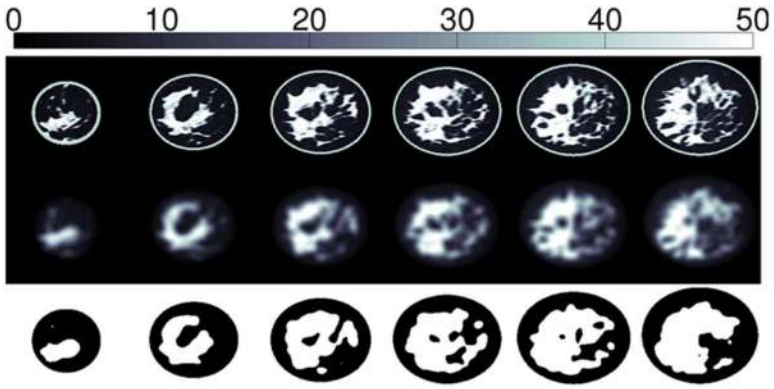

Fig. 1.

Cross-sections through *(top)* the 3-D profile of ε_s for a Class-III (heterogeneously dense) numerical breast phantom, *(middle)* the blurred 3-D distribution, and *(bottom)* the thresholded 3-D binary model. For the binary model, black corresponds to the portion to be printed in plastic, and white corresponds to the void. Adjacent cross sections are separated by 1 cm.

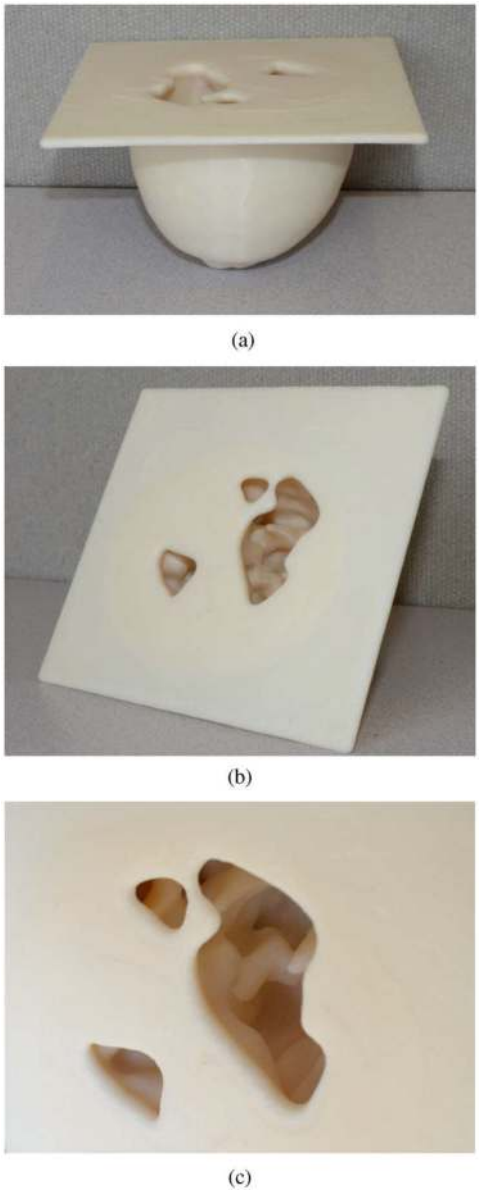

Fig. 2.

Photographs of the 3-D-printed breast phantom (prior to filling the fibroglandular void regions with liquid). (a) Side view shows the anthropomorphic exterior of the phantom with a support slab on top. (b), (c) Top views show the openings in the top slab, which reveal the heterogeneous interior (voids in regions corresponding to fibroglandular tissue, and plastic in regions corresponding to adipose tissue).

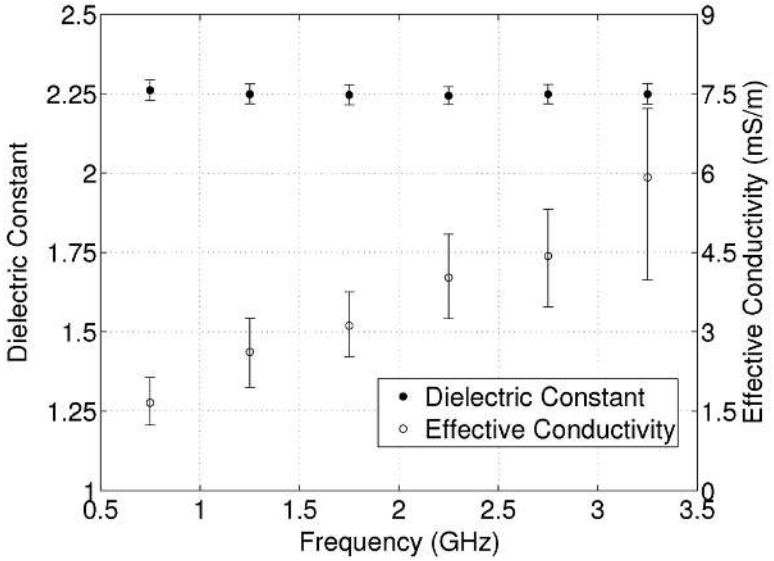

Fig. 3.
Measured dielectric constant and effective conductivity for 3-D-printed ABS plastic.